Bollettino di Geofisica Teorica ed Applicata Vol. 54, n. 3, pp. 271-282; September 2013
DOI 10.4430/bgta0075

Channel detection using instantaneous spectral attributes in one of the SW Iran oil fields

R. Mohebian, M. Yari, M.A. Riahi and R. Ghanati

Institute of Geophysics, University of Tehran, Iran

(Received: January 9, 2012; accepted: June 20, 2012)

ABSTRACT Instantaneous spectral attributes such as centre frequency and bandwidth are extracted from the time-frequency maps (spectrogram). These attributes are useful tools in interpretation of stratigraphic phenomena and detection of some geological events which normally cannot be observed in the conventional seismic sections, as river-buried channels. Channels filled with porous rocks and surrounded in a non-porous matrix play important role in stratigraphic explorations. Spectrograms are derived from spectral decomposition methods such as Short-Time Fourier Transforms (STFT), S-transform and Matching Pursuit Decomposition (MPD). STFT requires a predefined time window, which causes reduction of the time-frequency resolution. S-transform has better time-frequency resolution than STFT due to use of a varying-frequency window. Since MPD uses an iteration algorithm, so it is expected that instantaneous spectral attributes obtained from MPD have better time-frequency resolution than those from the other methods, though the iteration algorithm increases the time of computation in MPD. In this paper, we applied instantaneous centre frequency attribute from these methods to detect the channels in one of the SW Iran oil fields and then the results were compared with each other.

Key words: bandwidth, centre frequency, channels, matching pursuit, S-transform, Short-Time Fourier Transform.

1. Introduction

Channels play important role in stratigraphic explorations. Channels are often filled with porous sediments and surrounded in a non-porous matrix. These river-buried channels dominantly consist of sandstone. Thus, presence of a porous medium and a cap rock makes it possible to be as a suitable oil and gas reservoir. Instantaneous spectral attributes are used as a robust tool to describe the frequency-dependent characteristics of stratigraphic events. For instance, when a seismic signal is decomposed into a time-frequency map, time-varying frequency characteristics of the seismic signal are revealed. Various methods of spectral decomposition are employed in order to carry out interpretation and analysis of seismic data from geological phenomena.

The first method used is the Short Time Fourier Transform (STFT), in which a time-frequency spectrum is generated by taking Fourier transform over a preselected time window. (Peyton *et al.*,

1998; Partyka *et al.*, 1999). In this method, the use of a fixed time window leads to a decrease in the time-frequency resolution (Chakraborty and Okaya, 1995). Sinha *et al.* (2005) employed time-frequency continuous wavelet transform (TFCWT) based on continuous wavelet transform (CWT) to detect channels and low-frequency shadows of gas reservoirs. Stockwell *et al.* (1996) provided S-transform which is a useful tool to analyse the time-frequency distribution using a frequency-dependent window. The advantage of S-transform over STFT is that it utilizes a long time window for the low-frequency analysis and a shorter time window for the high-frequency analysis, and this property provides an optimum time-frequency resolution. Matos *et al.* (2005) studied the maximum peak frequencies estimated using S-transform to characterize the reservoir properties. This method, in addition to preserving of high frequency resolution, improves resolution of signals in the time domain. Among other methods of spectral decomposition, Matching Pursuit Decomposition (MPD) is another one, which its algorithm was first proposed by Mallat and Zhang (1993). This method has been used in order to detect thin layers (Marfurt and Kirlin, 2001), channels (Liu, 2006), and determine the hydrocarbon reservoirs limits (Wang, 2007). Instantaneous spectral attributes such as centre frequency, rms frequency, and bandwidth are derived using the definitions from probability theories (Barnes, 1993). These attributes can be estimated from time-frequency maps obtained using STFT, S-transform, and MPD methods.

In this study, we demonstrate how spectral decomposition methods such as STFT, S-transform, and MPD can be used to produce the instantaneous centre frequency. We initially investigate the algorithms of these three methods and then time-frequency resolutions from these methods on a synthetic trace are compared with each other. Next, we compare signal-frequency sections acquired from MPD on a real seismic data set in the frequencies of 20 Hz, 40 Hz and 60 Hz. At the end, we apply the centre frequency attribute extracted from three mentioned methods to detect the channels in one of the SW Iran oil fields.

2. Geological setting

The study area (Azadegan oil field) is located in the Abadan Plain in SW of Iran (Fig. 1). The Abadan Plain is considered a major oil province of Iran. The study area is about 23 km long and 9 km wide and its trend (N-S) is an exception to the belt of foothill fold of SW Iran, striking NW-SE. The Abadan Plain including this structure is situated within Mesopotamian foredeep basin in SW of the Zagros foreland and foredeep basin area contains many super giant oil and gas fields. Fig. 2 shows stratigraphic column of the study area and location of the Sarvak Formation as well as its neighbouring formations. The Sarvak Formation of the Bangestan Group is the most important oil reservoir in this region and is primarily composed of carbonate rocks. Based on Alavi (2004) studies, the Sarvak Formation is composed of grey, resistant (cliff-forming) shallow-marine limestones (partially argillaceous and micritic and partially sparry), including grainstone, rudist-bearing packstone, and stromatoporoid-bearing wackestone, with thin intercalated intervals of marl grading upwards to massive chalky limestone. The formation contains several river-buried channels which would certainly be interesting candidate to verify the utility of spectral decomposition methods. Since the channel thickness is inconsiderable compared to other geological events, utilizing time-frequency methods as well as time slices derived from these methods, we can better detect oil channels.

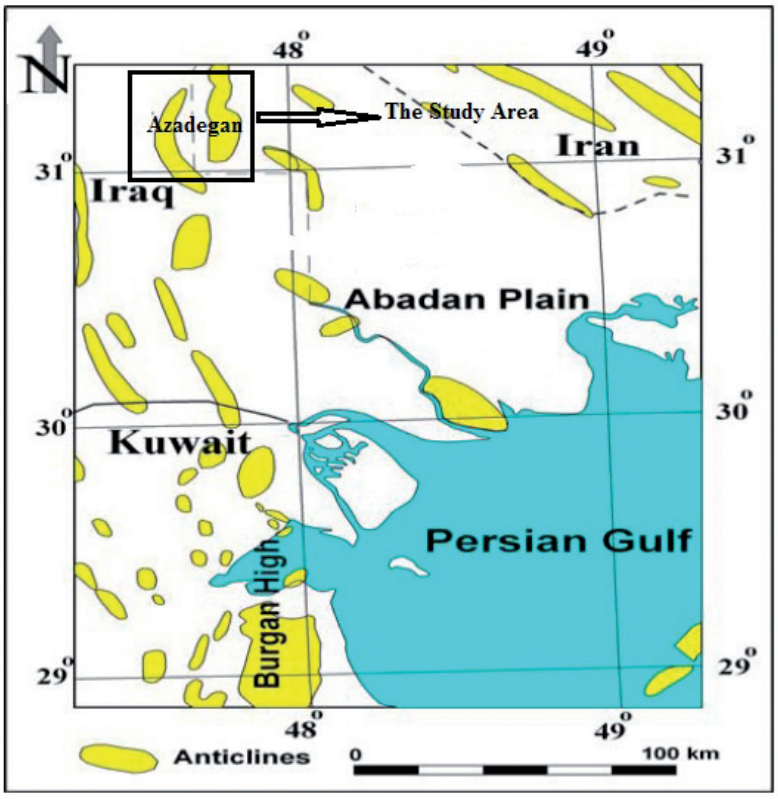

Fig. 1 - Location of the study area in the Abadan plain in SW of Iran (Abdollahi Fard *et al.*, 2002).

3. Time-frequency analysis

3.1. Short Time Fourier Transform

STFT uses a constant and arbitrary time-window $g(t)$ for the time-frequency analysis in which a real non-stationary signal is assumed as approximately stationary. STFT decomposes a semi-stationary signal $x(t)$ using a movable window $g(t)$ from different times τ into a 2D time-frequency $S(\tau, f)$, thus Fourier transform of the windowed signal, $x(t)g^*(t-\tau)$ yields STFT so that:

$$STFT_x(\tau, f) = \int_{-\infty}^{\infty} x(t)g^*(t-\tau)e^{-i2\pi ft}dt. \quad (1)$$

In time-frequency analysis, the objective is to have a window as small as possible to acquire a better resolution. On the other hand, Heisenberg uncertainty principle [Eq. (2)] limits the window's area:

$$\Delta t \Delta \omega \geq \frac{1}{2} \quad (2)$$

where, Δt is time-window length and $\Delta\omega$ is frequency-window length.

It means that one can only trade time resolution for frequency resolution, or vice versa. More important is that once the window has been selected for the STFT, then the time-frequency

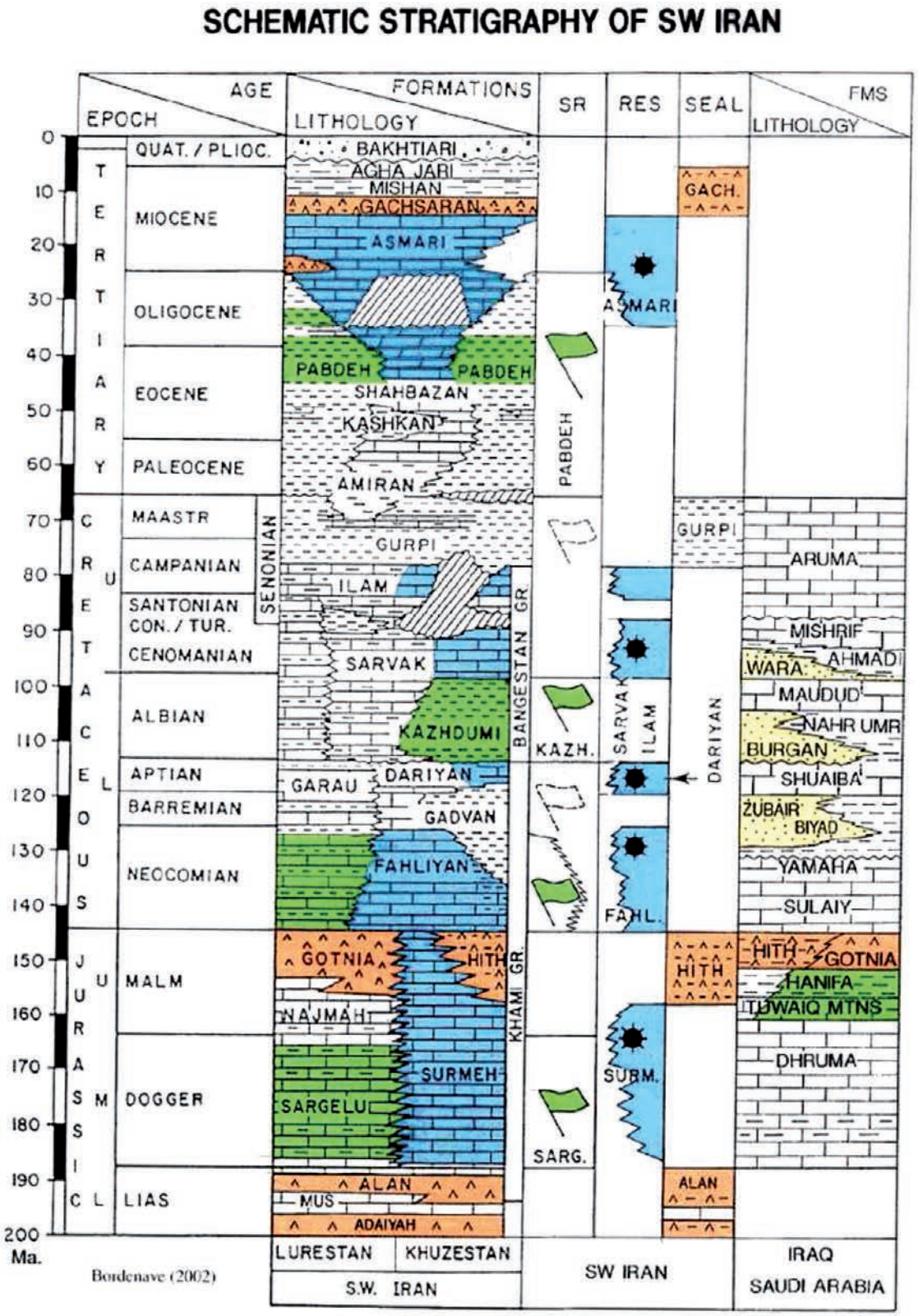

Fig. 2 - The stratigraphic column of the study area in southwest of Iran (Abdollahi Fard *et al*., 2002).

resolution is fixed over the entire time-frequency plane.

As mentioned above the STFT requires a fixed time window. In practice, seismic data are non-stationary and the STFT may not generate very reliable time-frequency map of it. Fixed window length and hence, fixed time-frequency resolution is a fundamental drawback with STFT (Chakraborty and Okaya, 1995). Fig. 3 shows time-frequency spectrum derived by STFT with the time window length of 1000 ms, 800 ms and 400 ms for a synthetic seismic trace. As demonstrated, STFT with the time window length of 400 ms provides better time-frequency resolution than the other time window lengths. As a result, we applied STFT with the time window length of 400 ms over the real data.

3.2. S-Transform

Morlet *et al*. (1982) have cross-correlated the complex wavelet W_M with input seismic trace $U(t)$ so that:

$$U_M(\tau, f) = \int u(t)\, W_M\, dt \tag{3}$$

where $U_M(\tau, f)$ is complex time-frequency spectrum and W_M is Morlet complex wavelet as follow:

$$W_M = e^{-(\tau - t)^2 f^2 \ln 2} e^{-i 2\pi f t}. \tag{4}$$

Stockwell *et al*. (1996) introduced an equation for S-transform so that:

$$U_S(\tau, f) = \int u(t) \frac{|f|}{\sqrt{2\pi}} e^{\frac{-(\tau - t)^2 f^2}{2}} e^{-i 2\pi f t} dt \tag{5}$$

where $U_S(\tau, f)$ is complex time-frequency spectrum, $U(t)$ is seismic trace, f is frequency, τ is transmission time, and t is time. S-transform decomposes a signal from time domain into time-frequency domain using a non-orthogonal Morlet wavelet with a varying size (Stockwell *et al*., 1996; Mallat, 1999). The difference between S-transform and STFT is that in STFT, the Gaussian window is a function of time, while in S-transform it is a function of time and frequency. Consequently, S-transform has higher time-frequency resolution in comparison with STFT. Fig. 3e shows the spectrogram from S-transform for a synthetic seismic trace. As demonstrated, S-transform results better time-frequency resolution compared to STFT with the time length of 400 ms.

3.3. Matching pursuit

MPD involves cross-correlation of a wavelet dictionary against the seismic trace. The projection of the best correlating wavelet on the seismic trace is then subtracted from that trace. The wavelet dictionary is then cross-correlated against the residual, and again the best correlating wavelet projection is subtracted. The process is repeated iteratively until the energy left in the residual fall below some acceptable threshold (Mallat and Zhang, 1993).

MPD expands a signal over a series of wavelets or atoms, selected from a dictionary composed of Gabor wavelet, supplemented with a canonical basis of discrete direct functions and the discrete Fourier basis of complex exponentials (Mallat and Zhang, 1993).

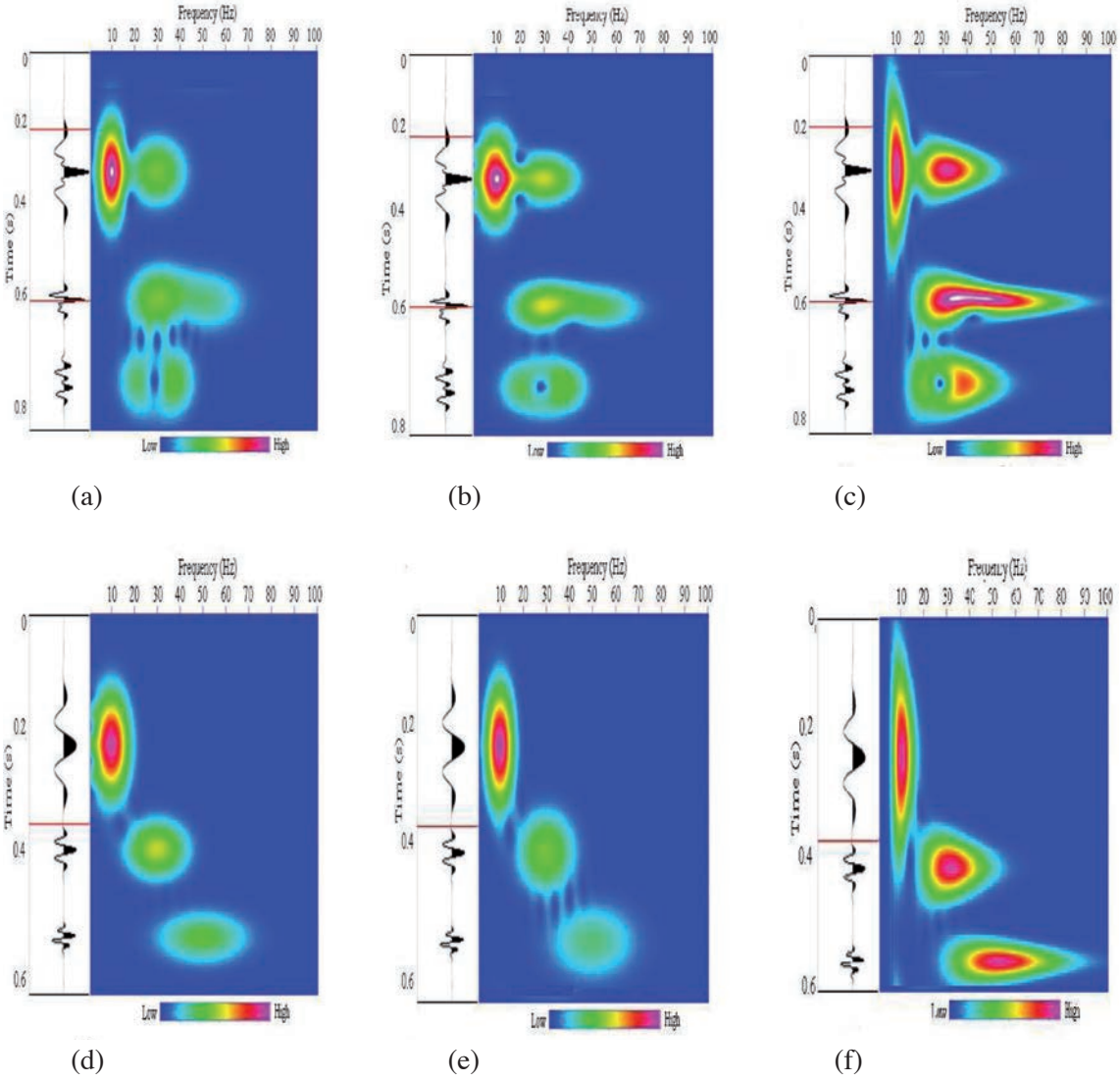

Fig. 3 - The comparison of time-frequency spectrum from spectral decomposition: panels a, b, and c, show time-frequency spectrum from STFT with the time window length of 1000 ms, 800 ms and 400 ms, respectively. As indicated, panel c associated with the time window length of 400 ms results in higher time-frequency resolution compared to panels a and c. Panels d, e and f demonstrate time-frequency spectrum from STFT (with the time window of 400 ms), S-transform and MPD, respectively. As illustrated, MPD exposes better timefrequency resolution than the other two methods.

A Gabor wavelet is a complex sinusoid function by a Gaussian envelope (Gabor, 1946), as the following equation:

$$g_{\gamma}(t) = w\left(\frac{t-u}{\sigma}\right)\exp\{i[\omega(t-u)+\phi]\} \tag{6}$$

where $w(t)$ is a Gaussian window, u is the time delay (translation), σ is the spread in the time axis (scale), ω is the centre frequency (modulation), and ϕ is the phase shift. In this paper, we applied Morlet wavelet. For seismic reflection signal analysis, use of Morlet wavelet is usually

preferred because the Morlet wavelet is suitable for energy and frequency quantification of seismic data and, particularly, is appropriate for attenuation and resolution studies of acoustic waves propagating through porous media.

A Morlet wavelet $m(t)$ centered at the abscissa u can be defined as (Morlet *et al.*, 1982):

$$m(t) = \exp\left[-\left(\frac{\ln}{\pi^2}\right) \div \frac{\omega_m{}^2 (t-u)^2}{\sigma^2}\right] \exp\{i[\omega_m (t-u) + \phi]\}, \tag{7}$$

where ω_m is the mean angular frequency, and σ is a constant value, which controls the wavelet width. Fig. 4 shows Morlet wavelet with 40 Hz dominant frequency in the frequency and time domain.

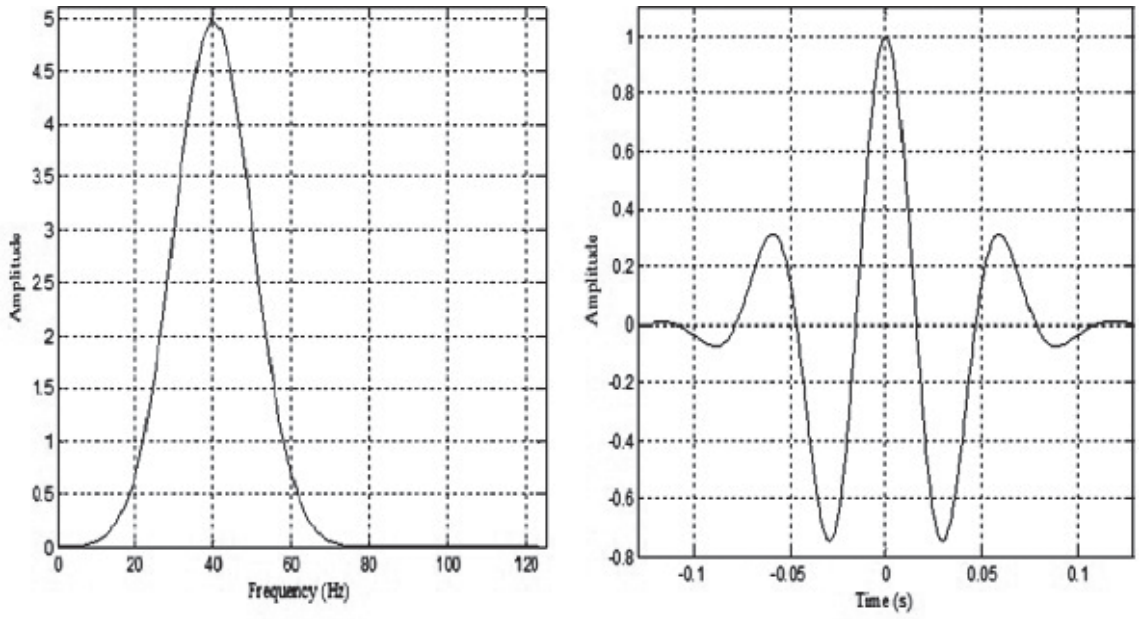

(a) (b)

Fig. 4 - Representation of Morlet wavelet with 40 Hz dominant frequency in a) frequency domain and b) time domain.

MPD is implemented iteratively, and any iteration adaptively extracts an optimal form wavelet g_{γ_n}, where n is the iteration number. After N iterations, a seismic trace $f(t)$ is expanded into the following form (Wang, 2007):

$$f(t) = \sum_{n=0}^{N-1} a_n g_{\gamma_n}(t) + R^{(N)} f \tag{8}$$

where a_n is the amplitude of the nth wavelet g_{γ_n}, $R^{(N)}f$ is the residual, and $R^{(0)}f = f$.

To achieve the time-frequency spectrum $f(t)$, the Wigner distribution is used and hence, the spectrum amplitude of its time-frequency is defined as follow:

$$Af(t,\omega)=\sum_{n=0}^{N-1}\frac{a_n}{\left\|g_{\gamma_n}\right\|}\left(\sqrt{\frac{\pi}{2\ln 2}}\frac{\sigma_n}{\omega_n}\right)^{\frac{1}{2}}\times\exp\left[-\left(\frac{\pi^2}{4\ln 2}\right)\frac{{\sigma_n}^2(\omega-\omega_n)^2}{{\omega_n}^2}\right]\times\exp\left[-\left(\frac{\ln 2}{\pi^2}\right)\frac{{\omega_n}^2(t-u_n)^2}{{\sigma_n}^2}\right] \quad (9)$$

where ω_n is the mean frequency of the *n*th wavelet, $\left\|g_{\gamma_n}\right\|$ is normalization factor derived from g_{γ_n}, and σ_n is the scale of the nth wavelet which controls the spread of wavelet.

The time-frequency spectrum of the mentioned synthetic seismic trace from MPD is presented in Fig. 3e. As seen, the time-frequency spectrum of MPD and S-transform display higher time-frequency resolution than STFT.

4. Instantaneous spectral attributes

In exploration seismology, instantaneous spectral attributes such as centre frequency, bandwidth and rms frequency can be obtained using definitions from probability theories.

Because of high sensitivity of frequency to the channels thickness, thus these attributes can be applied to highlight stratigraphic phenomena, as channels.

Fig. 5 illustrates these spectral measures with regard to the spectrum of a 30 Hz Ricker wavelet (Barnes, 1993).

Instantaneous power spectrum average is called instantaneous centre frequency and it is the first moment along the frequency axis of a time-frequency power spectrum (Barnes, 1993). Mathematically, it is presented by:

$$f_c(t)=\frac{\int_0^\infty f\left|E(t,f)\right|^2 df}{\int_0^\infty \left|E(t,f)\right|^2 df}\ , \quad (10)$$

where, f_c (t) denotes instantaneous centre frequency, and $E(t,f)$ is time-frequency spectrum which obtained from spectral decomposition methods (e.g., STFT, S-transform, and MPD). The square root of the second moment of time-frequency power spectrum along the frequency axis is called instantaneous rms frequency (Papoulis *et al.*, 2002); it is displayed as:

$$f_R^2(t)=\frac{\int_0^\infty f^2\left|E(t,f)\right|^2 df}{\int_0^\infty \left|E(t,f)\right|^2 df}\ , \quad (11)$$

where $f_R(t)$ is the instantaneous rms frequency, the standard deviation of the distribution about the instantaneous centre frequency is called instantaneous spectrum bandwidth ($f_{BW}(t)$), as the following:

$$f_{BW}^2(t)=\frac{\int_0^\infty (f-f_c)^2\left|E(t,f)\right|^2 df}{\int_0^\infty \left|E(t,f)\right|^2 df}\ . \quad (12)$$

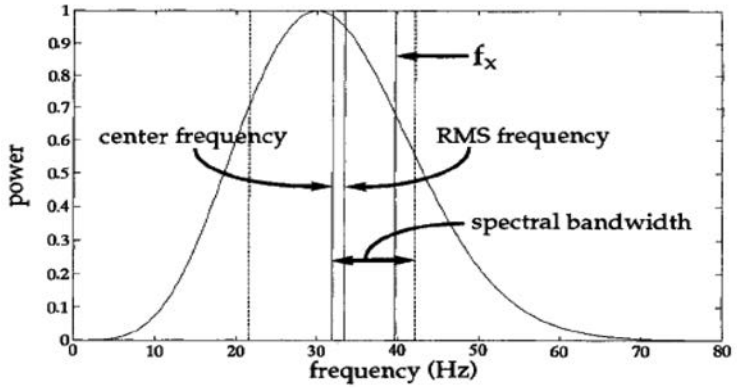

Fig. 5 - Power spectrum of a 30 Hz Ricker wavelet with a comparison of the centre frequency, the bandwidth, and the root-mean-square frequency.

5. An example from field data

In this paper, we used the data associated with one of the SW Iran oil fields to test the utility of instantaneous spectrum attributes in detection of the channels. The small thickness of such channels compared to other geological events is inconsiderable and hence, time slices are used to visualize the channels. In this study, we used the time slice at t=1.8 s which provided us with the best projection of the channels.

Fig. 6 shows the location of the channels in the seismic cross-section in which the both channel branches are traversed by the cross-line 327. It is displayed in Fig. 7a by line AB.

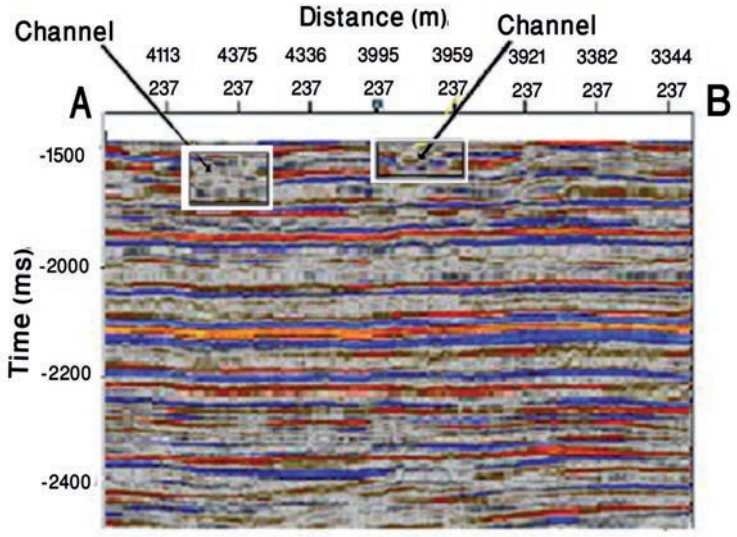

Fig. 6 - Seismic cross-section of the cross-line 327. Yellow arrows show the location of the two branches of the channel, this cross section is shown in Fig. 7 by line AB.

Fig. 7 shows single-frequency sections acquired from MPD in frequencies 20 Hz, 40 Hz and 60 Hz, respectively. As seen, in frequency 60 Hz, the minor branches of the channel, which have smaller thickness better, show up. While in frequency 20 Hz, the main branches of the channel more clearly show up.

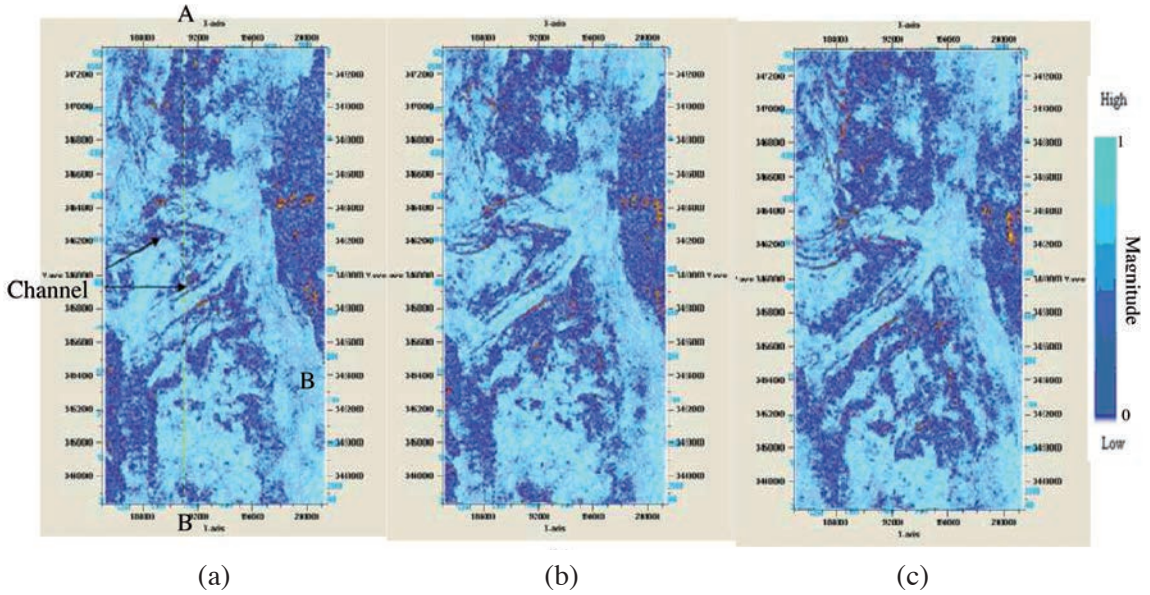

Fig. 7 - Cross-section in the time slice of 1.8 s extracted from 3D data for one of the SW Iran oil fields using MPD: a) 20 Hz; b) 40 Hz; c) 60 Hz. Channel branches are displayed by black arrows and line AB is related to cross-line 327 (Fig. 7a). In frequency 20 Hz, the minor branches of the channel having smaller thickness cannot transparently show up, while in frequencies 40 Hz and 20 Hz due to increase of frequency, the minor branches of the channel better show up.

Use of the single-frequency attribute sections provides a large volume of data, which makes the interpretation more complex. On the other hand, study of a particular horizon may lead to lose information of other horizons, while instantaneous spectrum attributes do not have such difficulties. These attributes illustrate the variation of frequency content of seismic data, thus thick and thin parts of a channel can be detected simultaneously. Fig. 8 shows the instantaneous centre frequency attributes obtained from STFT, S-transform and MPD in the time slice of 1.8 s, respectively.

As seen, S-transform better illustrates the channel branches, though STFT with an optimum window 400 ms relatively highlights the channels, but according to the fixed window length and Heisenberg uncertainty principle previously discussed, it has a lower time-frequency resolution. Also Fig. 8c shows the centre instantaneous frequency obtained from MPD. The arrows show the location of the channel branches. Due to an iteration algorithm which is used in MPD, as seen in Fig. 8c, it has better frequency resolution in comparison with the other two methods (STFT and S-transform).

6. Conclusions

In this paper, we first investigated various spectral decomposition methods such as STFT, S-transform and MPD. We then utilized single-frequency sections derived from MPD to detect channels, as illustrated the low frequencies better indicate the thick parts of the channel and the high frequencies show the thinner parts of the channel, while instantaneous spectral attributes can simultaneously reveal both the thick and thin parts of the channel. Finally, we studied the

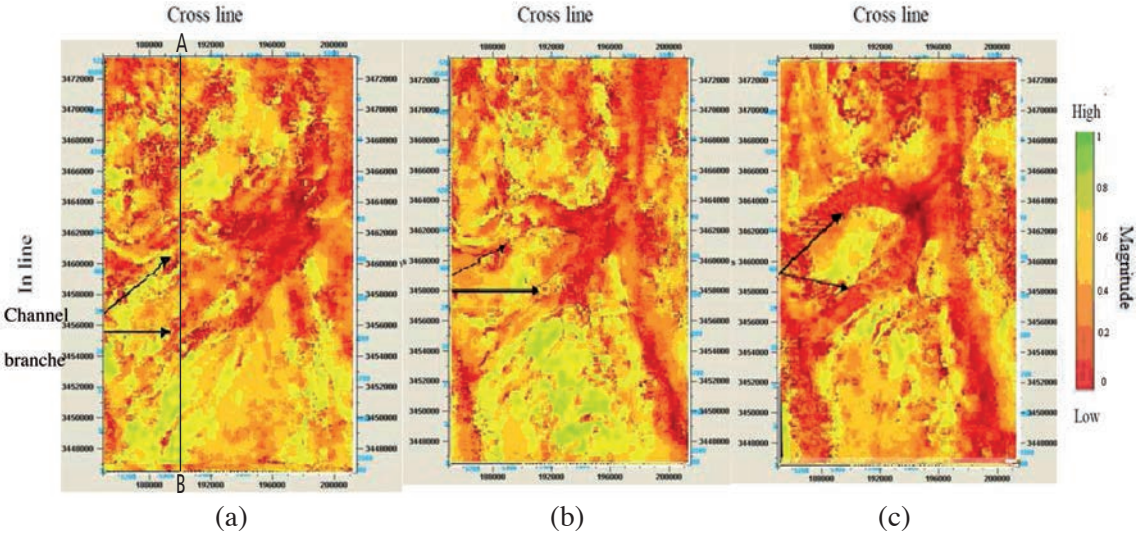

Fig. 8 - Cross-section of instantaneous centre frequency at t=1.8 s obtained by: a) STF with the time window length of 400 ms; b) S-transform; c) MPD. Channel branches are shown by the dark arrows and line AB represents cross line 327 (Fig. 8a). STFT due to use of a fixed time window cannot clearly detect the channel branches [(a)]. S-transform visualizes the channel branches better than STFT. Since MPD utilizes an iteration algorithm, it has better frequency resolution compared to the other two methods.

ability of instantaneous center frequency attribute extracted from STFT, S-transform and MPD to detect channels in one of the SW Iran oil fields. Computation of the time-frequency spectrum from STFT requires a predefined time window which leads to a stationary time-frequency resolution. Thus, this property is considered as a drawback with STFT. In contrast, S-transform due to use of varying-frequency window, gives a varied time-frequency resolution. As indicated, centre frequency attribute obtained from MPD visualizes the channel more transparently. It means that, this method has better time-frequency resolution and more efficiency compared to S-transform and STFT.

Acknowledgements. We would like to thank two anonymous reviewers and the publishing editor Dario Slejko for their comments that led to significant improvements in this paper.

REFERENCES

Abdollahi Fard I., Maleki M. and Aliee M.H.; 2002: *3D seismic interpretation and inversion of X field at Abadan plain (SW Iran)*. Geological Report, National Iranian Oil Company, Exploration Directorate, Geophysics Dpt.

Alavi M.; 2004: *Regional stratigraphy of the Zagros fold-thrust belt of Iran and its proforeland evolution*. Am. J. Sci., **304**, 1-20.

Barnes A.; 1993: *Instantaneous frequency and amplitude at the envelope peak of a constant-phase wavelet*. Geophys., **56**, 1058-1060.

Chakraborty A. and Okaya D.; 1995: *Frequency-time decomposition of seismic data using wavelet-based methods*. Geophys., **60**, 1906-1916.

Gabor D.; 1946: *Theory of communication*. J. Inst. Electrical Engineers, **93**, 429-457.

Liu J.; 2006: *Spectral decomposition and its application in mapping stratigraphy and hydrocarbons*. PhD Thesis, Department of Geosciences, University of Houston, TX, USA.

Mallat S.; 1999: *A wavelet tour of signal processing*. Academic Press, 2nd ed., San Diego, CA, USA, 629 pp.

Mallat S. and Zhang Z.; 1993: *Matching pursuits with time-frequency dictionaries*. IEEE Trans. Signal Process., **41**, 3397-3415.

Marfurt K.J. and Kirlin R.L.; 2001: *Narrow-band spectral analysis and thin-bed tuning*. Geophys., **66**, 1274-1283.

Matos M.C., Osorio P., Mundim E.C. and Moraces M.; 2005: *Characterization of thin beds through joint time-frequency analysis applied to a turbidite reservoir in Campos Basin, Brazil*. In: Proc. 75th SEG Annual Meeting, Houston, TX, USA, expanded abstracts, pp. 1429-1432.

Morlet J., Arens G., Fourgeau E. and Giard D.; 1982: *Wave propagation and sampling theory: Part I, Complex signal and scattering in multilayered media*. Geophys., **47**, 203-221.

Papoulis A.; 2002: *Probability random variables and stochastic processes (second edition)*. McGraw-Hill, New York, NY, USA, 576 pp.

Partyka G.A., Gridley J. and Lopez J.; 1999: *Interpretational applications of spectral decomposition in reservoir characterization*. The Leading Edge, **18**, 353-360.

Peyton L., Bottjer R. and Partyka G.; 1998: *Interpretation of incised valleys using new 3-D seismic techniques: a case history using spectral decomposition and coherency.* The Leading Edge, **17**, 1294-1298.

Sinha S., Routh R., Anno P. and Castagna J.; 2005: *Spectral decomposition of seismic data with continuous-wavelet transform*. Geophys., **70**, 19-25.

Stockwell R.G., Mansinha L. and Lowe R.P.; 1996: *Localization of the complex spectrum: the S-Transform*. IEEE Trans. Signal Process., **44**, 998-1001.

Wang Y.; 2007: *Seismic time-frequency spectral decomposition by matching pursuit*. Geophys., **72**, V13-V20.

Corresponding author: Reza Mohebian
Institute of Geophysics, University of Tehran
North Karegar Avenue, Tehran 1435944411, Iran
Phone: +98 21 61118219; fax: +98 21 88009560; e-mail: mohebian@ut.ac.ir